

Thymoquinone Blocks pSer/pThr Recognition by Plk1 Polo-Box Domain As a Phosphate Mimic

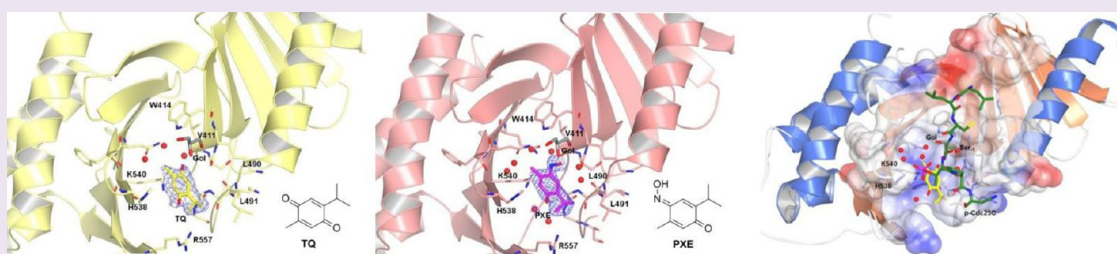
Zhou Yin,^{†,||} Yunlong Song,^{*,‡} and Peter H. Rehse^{*,§}

[†]School of Life Science and Technology, China Pharmaceutical University, 24 Tong Jia Xiang, Nanjing, Jiangsu 210009, China

[‡]Department of Medicinal Chemistry, School of Pharmacy, Second Military Medical University, 325 Guohe Road, Shanghai 200433, China

[§]Department of Biology, Shanghai Medicilon Inc., 585 Chuanda Road, Shanghai 201200, China

S Supporting Information



ABSTRACT: Phosphorylation-dependent protein–protein interaction has rarely been targeted in medicinal chemistry. Thymoquinone, a naturally occurring antitumor agent, disrupts prephosphorylated substrate recognition by the polo-box domain of polo-like kinase 1, a key mitotic regulator responsible for various carcinogenesis when overexpressed. Here, crystallographic studies reveal that the phosphoserine/phosphothreonine recognition site of the polo-box domain is the binding pocket for thymoquinone and its analogue poloxime. Both small molecules displace phosphopeptides bound with the polo-box domain in a slow but noncovalent binding mode. A conserved water bridge and a cation– π interaction were found as their competition strategy against the phosphate group. This mechanism sheds light on small-molecule intervention of phospho-recognition by the polo-box domain of polo-like kinase 1 and other phospho-binding proteins in general.

Thymoquinone (TQ) is the main therapeutic ingredient extracted from *Nigella sativa* with medical application for centuries.¹ Its antiproliferative effect covers a wide range of tumor cell lines and *in vivo* models.^{1–9} Its safety was underscored in the recent phase 1 clinical trial.¹⁰ Multiple molecular pathways have been proposed to account for TQ-induced apoptosis and cell cycle arresting at G₀/G₁,³ G₁,⁴ early G₁/S⁵, and G₂/M³ phases, involving mitotic regulators such as p53 protein, nuclear factor-kappa B and caspase-8.^{7–9} However, the molecular targets of TQ remained elusive until the polo-box domain (PBD) of polo-like kinase 1 (Plk1) was proposed.¹¹

Plk1 is an essential promoter of M phase progression, and its unchecked expression at G₂/M phase¹² leads to carcinogenesis in many TQ-sensitive tumor types.^{2,6,7,13} While a number of inhibitors were developed to disrupt the kinase domain of Plk1,¹⁴ its noncatalytic PBD emerged as an alternative target. PBD guides the catalytic domain to prephosphorylated substrates by recognizing a Ser-pSer/pThr core motif,¹⁵ and as shown by Reindl et al.,¹¹ TQ disrupts this process, delocalizes Plk1, and eventually arrests the cell cycle.

Though a few nonpeptidic inhibitors against Plk1-PBD have been identified,^{11,16,17} how TQ or any of them blocks the phospho-substrate recognition remained unknown due to the undetermined inhibitor binding site and the mechanism.^{11,18} Covalent modification was proposed based on the on-set time

dependency of TQ¹¹ and the fact that the quinone ring has Michael acceptor carbons capable of reacting with thiol groups on surface cysteine residues.

Moreover, Reindl et al. found the multiple targeting of phospho-recognition proteins by TQ, including Chk2 FHA domain and Pin1 WW domain, which recognize pSer/pThr motif and Src homology 2 (SH2) domain of STAT3, which binds to pTyr epitope.¹¹ This may suggest a specific binding mode of TQ to phospho-recognition sites. Targeting phospho-signaling by blocking pTyr recognition remains challenging to date.¹⁹ Besides, there's no definitive mechanistic elucidation to the small-molecule inhibition of PBD, one of the rarely tapped pSer/pThr binding domains. Structural evidence of TQ inhibiting phospho-recognition by Plk1 PBD may explain the time-dependency and reveal a mechanism of small molecule intervention of phospho-recognition.

In this work, we present a TQ-complexed Plk1-PBD crystal structure (PBD^T, 2.75 Å; crystallographic data in Supplementary Table S1). We tried to soak poloxin, a known Plk1-PBD inhibitor,¹¹ into PBD crystals but only found electron density for the oxime fragment of poloxin (PBD^P, 1.93 Å; crystallo-

Received: August 17, 2012

Accepted: November 7, 2012

Published: November 7, 2012

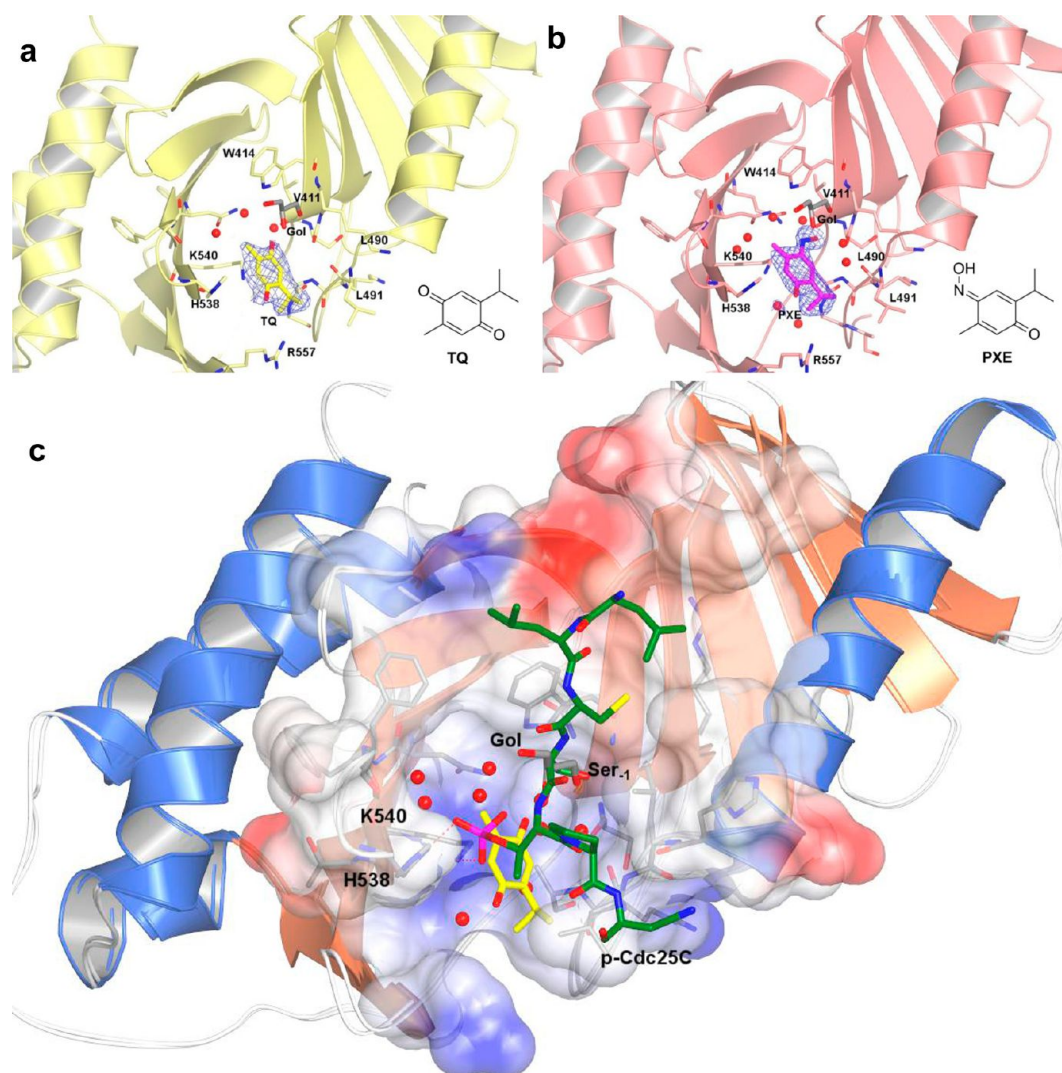


Figure 1. (a,b) Ribbon diagram of PBD^T chain A (lemon) and PBD^P chain A (pink). Residues around TQ (yellow) and PXE (magenta) are presented. Glycerol molecules are shown in gray and water molecules as red balls. 2mFo-DFc electron density maps (blue wire mesh) of TQ and PXE are contoured at 1 σ . (c) PBD^T chain A is superimposed onto Protein Data Bank entry 3BZI, both colored by secondary structure (α -helix, blue; β -sheet, coral; and others, white). TQ (yellow) and a glycerol molecule (gray) are shown. The phosphopeptide in 3BZI is shown in dark green (noncarbon atoms are colored as N, blue; O, red; and P, magenta). Hydrogen bonds between the phosphate and the Lys540–His538 pincer are shown in dotted lines. Red balls represent water molecules in 3BZI.

graphic data in Supplementary Table S1). We therefore named this TQ analogue poloxime (PXE), a combination of poloxin and oxime. As expected, PXE is a hydrolysis product of poloxin, confirmed with liquid chromatography–mass spectrometry (Supplementary Figure S1a–b). The lower occupancy of PXE may explain its higher B-factor than that of TQ (Supplementary Table S1). We further determined a native PBD crystal structure (PBD^{ApO}, 1.95 Å; crystallographic data in Supplementary Table S1).

PBD^T and PBD^P pinpointed the inhibitor binding site: the phosphate group recognition site between the two polo boxes of the PBD, each consisting of an α helix and a β sheet (Figure 1a,b). This pocket consists of a hydrophobic half (Val411, Trp414, Leu490, and Leu491) and a positively charged half (His538, Lys540, and Arg557) where the Lys540–His538 pincer clinches phosphopeptides by the phosphate (Figure 1c).²⁰ A glycerol molecule is found near the bound ligands, occupying the Ser-1 position for phosphopeptide binding, which is observed in other PBD crystal structures as well.¹⁵

Prephosphorylation of Plk1 substrates (e.g., p-Cdc25c, Figure 1c) is critical for the PBD recognition^{15,20} and accounts for superior binding affinity by several orders of magnitude compared to their nonphosphorylated versions, which was found almost nonbinding by Huggins et al. using isothermal titration calorimetry.²¹ However, a PBD crystal structure with a nonphosphorylated peptide is available.¹⁴ This can be explained by the law of mass: the cocrystallography is done with high concentrations of both the protein and the peptide. Since the phosphate group functions as a turnkey in phosphorylation-dependent signaling pathways, the PBD^T structure suggests that TQ jams the keyhole, preventing Plk1 from recognizing its mitotic substrates via PBD, and may subsequently promote cell-cycle arrests and apoptosis. This corroborates with the G₂/M phase arrests in both TQ-centered³ and Plk1-centered studies.¹²

The binding of TQ and PXE has no apparent disruption of PBD compared to the native structure except for a ~ 2 Å positional shift in Leu491 side chain (arrow, Figure 2a,b). In

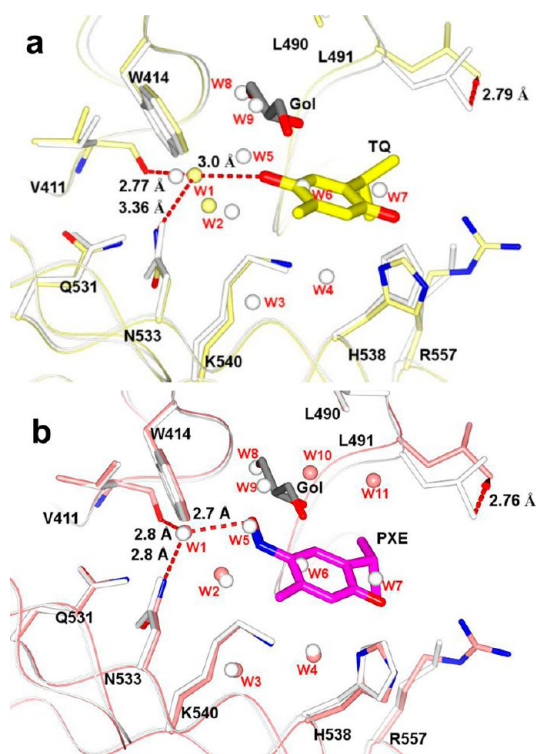


Figure 2. (a,b) TQ (yellow) and PXE (magenta) in contact with a structural water (W1), respectively. TQ/PXE-bound structures (lemon and pink) are superimposed onto PBD^P chain B (white) as a native structure. Atoms are colored by model except noncarbon atoms of the PBD^T/PBD^P side chains (N, blue; O, red). Glycerol molecules are CPK colored. Hydrogen bonds are given as red dashed lines. Arrows show the shift of Leu491.

fact, the entire Leu491–Leu492 backbone was slightly pushed away to allow entry of two interfacial water molecules (W8 and W9) in PBD^P or PBD^T. Lys540 has close contact with both ligands, while the imidazole ring of His538 is slightly turned but not close enough (>3.5 Å to the nearest carbon of TQ/PXE) to make interaction. What's more, we found the pocket extensively hydrated by crystallographic water molecules (W1–W11, Figure 2a,b), which makes no extra space for bulk solvent (Supplementary Figure S3a). The binding of TQ/PXE is in effect a displacement of several crystallographic waters (W5–7). When bound, PXE is buried in a network of structural waters (Supplementary Figure S3c), which should be the same case of TQ binding, but water molecules can hardly be identified due to the lower resolution (Supplementary Figure S3b).

Reindl et al. did not observe a covalently bound inhibitor to PBD with mass spectrometry so as to explain time-dependent inhibition.¹¹ Neither does TQ/PXE have covalent bonds with PBD as shown by the crystal structures nor do they mimic a charged phosphate. The question becomes what directed the binding of TQ/PXE to the phosphate binding site and why time-dependency. A fluorescence polarization based assay¹¹ was used to characterize TQ and PXE's binding kinetics by tracing the unbound PBD with fluorescently labeled phosphopeptide. The IC_{50} values of both TQ and PXE inhibiting the phosphopeptide binding were tracked (Supplementary Figure S2). The dropping of IC_{50} s slowed down remarkably after a quick slump, and the Hill slope values were converging to 1 (Supplementary Table S2a,c). These indicate competitive

binding instead of inactivation due to covalent modification. We initiated dissociation of preincubated TQ/PXE-PBD with dithiothreitol, which neutralizes TQ and PXE containing Michael acceptors. However, due to the limited time frame, we were not able to see complete dissociation of PXE, while TQ did not display significant dissociation (Supplementary Table S2b,d). The dissociation of PXE casts doubt on covalent modification and supports competitive binding as a viable theorem. The glycerol molecule adjacent to TQ and PXE has contacts with both ligands, but glycerol, up to 30% in the buffer, had no effect in neither the peptide binding nor the TQ/PXE inhibition (data not shown).

A recent study of shielded hydrogen bonds as the determinant of binding kinetics may uncover the mechanism of the slow binding of TQ and PXE.²² In their work, the almost buried polar atoms (ABPA) of the receptor are found responsible of slow ligand binding as the solvent accessible surface area of the ABPA (A_0) is less than 10 Å², and the binding site is concave ($\Delta A < 0$; A_0 decreases as the probe size increases). Such slow-dissociating ligand–receptor pair is exemplified by biotin–streptavidine of which the dissociation rate constant can be 100-fold smaller²³ than that of TQ–PBD, presumably because of those water-shielded hydrogen bonds.

The structural feature of the PBD binding pocket is a similar case as a structural water (W1, Figure 2) serves as an ABPA ($A_0 = 2.96$ Å², $\Delta A < 0$), which, once with a hydrogen bond with TQ/PXE, is completely shielded from bulk solvent ($A_0 = 0$). The V-shaped concave pocket only allows the presence of a few adjacent crystallographic waters (W2, W8, and W9), thus greatly reducing any dielectric effect by bulk solvent and strengthening the hydrogen bonding between the W1 and TQ/PXE. Both the narrow pocket and TQ/PXE are steric impediment themselves, preventing bulk solvent from coming in to contact with W1 before ligand dissociation. Similarly, the kinetic barrier of TQ/PXE association should largely come from the dissociation of W5, which shields W1 from bulk solvent as well. In fact, as aforementioned, the narrow and deep pocket does not have space for bulk solvent at all (Supplementary Figure S3a), which means all three structural water molecules (W5–W7, Figure 2a,b) have to dissociate before TQ/PXE can access it; accordingly, TQ/PXE has to move out of the pocket before water can refill it. Such empty-pocket transition state must be energetically unfavorable and kinetically penalized. Consistently, because of the smaller size of water than TQ/PXE, steric impediment is less significant for water, which explains the much slower dissociation of TQ/PXE than their respective association.

In addition, we assessed the mobility of crystallographic waters with a 6 ns molecular dynamics simulation to verify the role of W1 as a structural water that needs to be treated as a part of the receptor. We tracked the trajectory and found W1 showing little movement during the first 4 ns, together with another 2 waters below 3 Å of root-mean-square fluctuation (RMSF) (Figure 3a). W1, the only conserved water in the phosphate binding pocket, oscillated between Asn533ND2 (a hydrogen donor) and Val411O (a hydrogen acceptor). Their bond lengths are demonstrated in the plot of radial distribution function (RDF): the red peak (2.75 Å) for the most-likely distance between W1O and Val411O, and the blue peak (3.15 Å) for that of W1O and Asn533ND2 (Figures 3b,c). Such arrangement enables W1 to bridge the binding of either a hydrogen acceptor (carbonyl O7 of TQ) or a potential hydrogen donor (PXE's oxime O13): W1 makes two hydrogen

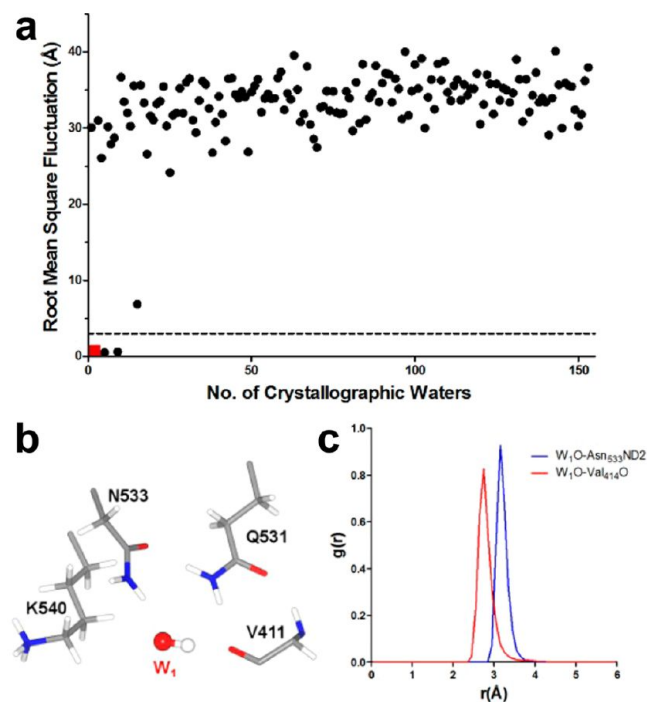


Figure 3. (a) Root-mean-square fluctuation of crystallographic waters averaged over the first 4 ns simulation. Dashed line represent $y = 3.0$. W_1 is shown as a red square. (b) W_1 (as ball and stick) and nearby residues (as cylinders), added with hydrogen and energetically minimized. Atoms are CPK colored. Blue and red dashed lines represent hydrogen bonds between W_1 and Asn533/Val411, respectively, of which the lengths are plotted as a radial distribution function in panel c, where the blue and red curves peak at the most probable radius within the 4 ns.

bonds in both cases, one with the receptor, the other with the ligand. Additionally, W_1 is buried deeply in the pocket and not available in phosphopeptide positioning. TQ/PXE are capable of penetrating the hydrogen bond network made by crystallographic waters by slowly displacing them and eventually anchor themselves on the conserved W_1 , while a phosphate group can only recruit waters with much higher mobility.²¹

Both TQ and PXE lack the negative charges of a phosphate group, which allows it to be attracted by the protonated Lys540. They nevertheless overlap with the phosphate when the protein structures are superimposed and are particularly close to Lys540. We suspected there is a cation- π interaction between the protonated lysine $N\zeta^+$ and TQ/PXE's cross-conjugated systems, which may represent another strategy for the small molecules to compete with phosphopeptides.

Since the current molecular mechanics force fields do not explicitly account for cation- π interaction and are likely the cause of both TQ and PXE being drawn to Arg557 during MD simulations of PBD^T and PBD^P, respectively (data not shown), we turn to quantum mechanical calculations to see if TQ or PXE nevertheless make use of the Lys540 albeit lacking net negative charges. Lys540 $N\zeta^+$ is located on top of C_6 in the TQ/PXE-bound structures, and thus, $N\zeta^+-C_6$ is nearly vertical to the $-C_2=C_1-C_6=O_7/N_7-$ plane (Figure 4a,b). Considering that C_6 is a local geometric center of the cross-conjugated systems consisting two alkenes ($C_4=C_5$ and $C_1=C_2$), and a carbonyl/oxime group, $N\zeta^+$ is on a favorable spot for making cation- π interaction. We did ab initio quantum mechanical calculations of interaction energy, defined as the energetic

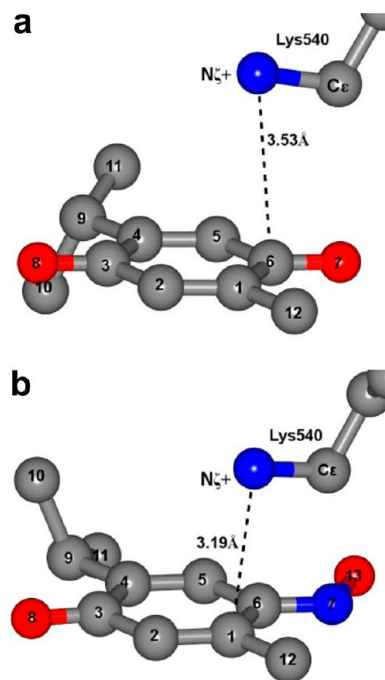


Figure 4. Shortest intermolecular distances between Lys540+ and TQ(a)/PXE(b) are represented as dashed lines. Atoms are CPK colored.

difference between the complex (E_{complex}) and the monomers (E_{ligand} and E_{protein}), at Hartree-Fock (HF) and the MP2 levels using 6-31G* (0.25) and 6-311+G(**) basis sets. The basis set superposition error (BSSE) was corrected using the Boys and Bernardi counterpoise method.²⁴ The calculated interaction energies (Table 1) are of significant magnitude, suggesting that

Table 1. MP2 Calculated Interaction Energies (kcal/mol)

	ΔE_{HF}^a	ΔE_{MP2}^a	E_{corr}^b
Lys540-TQ			
6-31G*(0.25)	-0.89	-6.52	-5.63
6-311+G(**)	-0.30	-5.77	-5.47
Lys540-PXE			
6-31G*(0.25)	-0.09	-8.37	-8.28
6-311+G(**)	0.72	-7.62	-8.34

^aGas-phase intermolecular interaction energies (in kcal/mol) at the MP2 level (ΔE_{MP2}) and HF level (ΔE_{HF}) after BSSE correction. ^bThe dispersion energy was defined as $E_{\text{corr}} = \Delta E_{\text{MP2}} - \Delta E_{\text{HF}}$.

the protonated Lys540 remarkably stabilizes TQ/PXE-PBD complexes. Comparison of MP2 and HF interaction energies shows a substantial correlation correction, which indicates that, in addition to electrostatic interactions, dispersion energies (electron correlation effect) contribute substantially to the cation- π interaction. The reduced dielectric effect due to the lack of nearby bulk solvent should be favorable of such interaction. This solvent shielded interaction should have a similar effect to the binding kinetics just as the solvent shielded hydrogen bond.

A number of phospho-recognition proteins have emerged with a variety of functions with regard to phosphorylation-dependent signaling and cell cycle control, including 14-3-3,²⁵ BRCA1 carboxyl terminal domains,²⁶ FHA domains,²⁷ and the aforementioned Pin1 and Plk1-PBD domains, which TQ binds to. Since these pSer/pThr binding proteins have lysine and/or

arginine in their phospho-recognition pockets as Plk1 PBD does,²⁰ such cation- π interaction may be a general phenomenon and explains the nonspecificity of TQ.

Although having potentially reactive α,β -unsaturated carbons, TQ is the only small-molecule inhibitor of pSer/pThr/pTyr recognition with actual therapeutic application in intervening cell cycle signaling to our knowledge. Unlike phosphonate, sulfonate, or carboxylic compounds as phosphate mimics, which have poor membrane permeability, TQ is moderately hydrophobic and bears zero net charge, yet utilizing the targets' structural features for phosphate-binding just the same. In fact, other PBD inhibitors may use the same strategy since they have substructures that resemble TQ. A pan-specific PBD inhibitor¹⁶ has a cross-conjugated hexatomic ring system with a carbonyl terminus and a large group similar to the isopropyl group of TQ. Purpurogallin,¹⁷ another PBD inhibitor with a cross-conjugated system in a heptatomic ring, similarly has a carbonyl terminus and a combined ring at the position of the isopropyl group of TQ. They could adopt the same orientation of TQ/PXE when binding to PBD and have interactions with the structural water and the Lys540. As the candidate pool of PBD inhibitors expands, we will learn more about the structural basis of phospho-recognition inhibition of PBD. The complex structures herein offer a new perspective of the energetic nature of TQ/PXE's competition of phosphopeptide binding to Plk1 PBD. The phospho-mimicry mechanism may benefit medicinal design targeting PBD and other phospho-binding domains in general.

METHODS

Plk1-PBD constructs, residue range 326–603 for assay and residue range 367–603 for crystallography, were cloned, expressed, and purified. Crystallization was carried out by vapor diffusion at 18 °C in 1.4 M sodium potassium tartrate, 50 mM MES, pH 6.5, and 100 mM Hepes, pH 6.0. TQ/PXE were soaked into the crystals. Diffraction data sets were collected at wavelength 0.98 Å, 100 K, at the Beamline 17U, Shanghai Synchrotron Radiation Facility (SSRF). Structure was solved by molecular replacement using Protein Data Bank entry 1UMW as the search model. Data collection and refinement statistics are reported in Supplementary Table S1. Full details are given in the Supporting Information.

ASSOCIATED CONTENT

Supporting Information

Crystallographic data, biochemistry, analytical chemistry, supplementary figures and table, detailed materials and methods. This material is available free of charge via the Internet at <http://pubs.acs.org>.

Accession Codes

The atomic coordinates and structure factors of PBD^{APO}, PBD^P, and PBD^T were deposited under accession codes 4HSX, 4H71, and 4HCO, respectively.

AUTHOR INFORMATION

Corresponding Author

*E-mail: ylsong@smmu.edu.cn (Y.S.); peter.rehse@mediciloninc.com (P.H.R.).

Present Address

^{||}School of Chemistry, University of Wollongong, Northfields Avenue, Wollongong, NSW 2522, Australia.

Notes

The authors declare no competing financial interest.

ACKNOWLEDGMENTS

We thank the staff at the Beamline 17U, Shanghai Synchrotron Radiation Facility (SSRF), and Shanghai Supercomputer Center. This work is cosponsored by China Pharmaceutical University and Shanghai Medicilon Inc. We are grateful to Shanghai Medicilon Inc. for financial and technological support.

REFERENCES

- (1) Trang, N. T.; Wanner, M. J.; Phuong, L. V. N.; Koomen, G. J.; and Dung, N. X. (1993) Thymoquinone from eupatorium ayapana. *Planta Med.* 59, 99.
- (2) Banerjee, S.; Kaseb, A. O.; Wang, Z.; Kong, D.; Mohammad, M.; Padhye, S.; Sarkar, F. H.; and Mohammad, R. M. (2009) Antitumor activity of gemcitabine and oxaliplatin is augmented by thymoquinone in pancreatic cancer. *Cancer Res.* 69, 5575–5583.
- (3) Gali-Muhtasib, H. U.; Abou Kheir, W. G.; Kheir, L. A.; Darwiche, N.; and Crooks, P. A. (2004) Molecular pathway for thymoquinone-induced cell-cycle arrest and apoptosis in neoplastic keratinocytes. *Anticancer Drugs* 15, 389–399.
- (4) Alhosin, M.; Abusnina, A.; Achour, M.; Sharif, T.; Muller, C.; Peluso, J.; Chataigneau, T.; Lugnier, C.; Schini-Kerth, V. B.; Bronner, C.; and Fuhrmann, G. (2010) Induction of apoptosis by thymoquinone in lymphoblastic leukemia jurkat cells is mediated by a p73-dependent pathway which targets the epigenetic integrator uhrf1. *Biochem. Pharmacol.* 79, 1251–1260.
- (5) Wafaa, A. A.; Sohair, A. H.; Fayek, M. G.; Maha, A. E. T.; and Farid, A. A. B. (2008) The *in vitro* promising therapeutic activity of thymoquinone on hepatocellular carcinoma (hepg2) cell line. *Global Vet.* 2, 233–241.
- (6) Kaseb, A. O.; Chinnakannu, K.; Chen, D.; Sivanandam, A.; Tejawani, S.; Menon, M.; Dou, Q. P.; and Reddy, G. P. (2007) Androgen receptor and e2f-1 targeted thymoquinone therapy for hormone-refractory prostate cancer. *Cancer Res.* 67, 7782–7788.
- (7) Gali-Muhtasib, H.; Diab-Assaf, M.; Boltze, C.; Al-Hmaira, J.; Hartig, R.; Roessner, A.; and Schneider-Stock, R. (2004) Thymoquinone extracted from black seed triggers apoptotic cell death in human colorectal cancer cells via a p53-dependent mechanism. *Int. J. Oncol.* 25, 857–866.
- (8) Sethi, G.; Ahn, K. S.; and Aggarwal, B. B. (2008) Targeting nuclear factor-kappa b activation pathway by thymoquinone: Role in suppression of antiapoptotic gene products and enhancement of apoptosis. *Mol. Cancer Res.* 6, 1059–1070.
- (9) El-Mahdy, M. A.; Zhu, Q.; Wang, Q. E.; Wani, G.; and Wani, A. A. (2005) Thymoquinone induces apoptosis through activation of caspase-8 and mitochondrial events in p53-null myeloblastic leukemia hl-60 cells. *Int. J. Cancer* 117, 409–417.
- (10) Al Amri, A. M.; and Bamosa, A. O. (2009) Phase I safety and clinical activity study of thymoquinone in patients with advanced refractory malignant disease. *Shiraz Med. J.* 10, 107–111.
- (11) Reindl, W.; Yuan, J.; Kramer, A.; Strebhardt, K.; and Berg, T. (2008) Inhibition of polo-like kinase 1 by blocking polo-box domain-dependent protein-protein interactions. *Chem. Biol.* 15, 459–466.
- (12) Martin, B. T.; and Strebhardt, K. (2006) Polo-like kinase 1: Target and regulator of transcriptional control. *Cell Cycle* 5, 2881–2885.
- (13) Chopra, P.; Sethi, G.; Dastidar, S. G.; and Ray, A. (2010) Polo-like kinase inhibitors: An emerging opportunity for cancer therapeutics. *Expert Opin. Invest. Drugs* 19, 27–43.
- (14) Garcia-Alvarez, B.; de Carcer, G.; Ibanez, S.; Bragado-Nilsson, E.; and Montoya, G. (2007) Molecular and structural basis of polo-like kinase 1 substrate recognition: Implications in centrosomal localization. *Proc. Natl. Acad. Sci. U.S.A.* 104, 3107–3112.
- (15) Yun, S. M.; Moulaei, T.; Lim, D.; Bang, J. K.; Park, J. E.; Shenoy, S. R.; Liu, F.; Kang, Y. H.; Liao, C.; Soung, N. K.; Lee, S.; Yoon, D. Y.; Lim, Y.; Lee, D. H.; Otaka, A.; Appella, E.; McMahon, J. B.; Nicklaus, M. C.; Burke, T. R., Jr.; Yaffe, M. B.; Wlodawer, A.; and Lee, K. S. (2009) Structural and functional analyses of minimal phosphopeptides

targeting the polo-box domain of polo-like kinase 1. *Nat Struct Mol Biol* 16, 876–882.

(16) Reindl, W., Yuan, J., Kramer, A., Strebhardt, K., and Berg, T. (2009) A pan-specific inhibitor of the polo-box domains of polo-like kinases arrests cancer cells in mitosis. *ChemBioChem* 10, 1145–1148.

(17) Watanabe, N., Sekine, T., Takagi, M., Iwasaki, J., Imamoto, N., Kawasaki, H., and Osada, H. (2009) Deficiency in chromosome congression by the inhibition of plk1 polo box domain-dependent recognition. *J. Biol. Chem.* 284, 2344–2353.

(18) Liao, C., Park, J. E., Bang, J. K., Nicklaus, M. C., and Lee, K. S. (2010) Exploring potential binding modes of small drug-like molecules to the polo-box domain of human polo-like kinase 1. *ACS Med. Chem. Lett.* 1, 110–114.

(19) Zhang, X., He, Y., Liu, S., Yu, Z., Jiang, Z. X., Yang, Z., Dong, Y., Nabinger, S. C., Wu, L., Gunawan, A. M., Wang, L., Chan, R. J., and Zhang, Z. Y. (2010) Salicylic acid based small molecule inhibitor for the oncogenic src homology-2 domain containing protein tyrosine phosphatase-2 (shp2). *J. Med. Chem.* 53, 2482–2493.

(20) Elia, A. E., Rellos, P., Haire, L. F., Chao, J. W., Ivins, F. J., Hoepker, K., Mohammad, D., Cantley, L. C., Smerdon, S. J., and Yaffe, M. B. (2003) The molecular basis for phosphodependent substrate targeting and regulation of plks by the polo-box domain. *Cell* 115, 83–95.

(21) Huggins, D. J., McKenzie, G. J., Robinson, D. D., Narvaez, A. J., Hardwick, B., Roberts-Thomson, M., Venkitaraman, A. R., Grant, G. H., and Payne, M. C. (2010) Computational analysis of phosphopeptide binding to the polo-box domain of the mitotic kinase plk1 using molecular dynamics simulation. *PLoS Comput Biol* 6, e1000880.

(22) Schmidtke, P., Luque, F. J., Murray, J. B., and Barril, X. (2011) Shielded hydrogen bonds as structural determinants of binding kinetics: Application in drug design. *J. Am. Chem. Soc.* 133, 18903–18910.

(23) Piran, U., and Riordan, W. J. (1990) Dissociation rate constant of the biotin–streptavidin complex. *J. Immunol. Methods* 133, 141–143.

(24) Boys, S. F., and Bernardi, F. (1970) *Mol. Phys.* 19, 553–566.

(25) Zhao, J., Du, Y., Horton, J. R., Upadhyay, A. K., Lou, B., Bai, Y., Zhang, X., Du, L., Li, M., Wang, B., Zhang, L., Barbieri, J. T., Khuri, F. R., Cheng, X., and Fu, H. (2011) Discovery and structural characterization of a small molecule 14-3-3 protein–protein interaction inhibitor. *Proc. Natl. Acad. Sci. U.S.A.* 108, 16212–16216.

(26) Shao, Z., Li, F., Sy, S. M., Yan, W., Zhang, Z., Gong, D., Wen, B., Huen, M. S., Gong, Q., Wu, J., and Shi, Y. (2012) Specific recognition of phosphorylated tail of h2ax by the tandem brct domains of mcph1 revealed by complex structure. *J. Struct. Biol.* 177, 459–468.

(27) Mahajan, A., Yuan, C., Lee, H., Chen, E. S., Wu, P. Y., and Tsai, M. D. (2008) Structure and function of the phosphothreonine-specific fha domain. *Sci. Signaling* 1, re12.